NASA/TM—2010-216342/REV1

Microstructural Characterization of Metal Foams: An Examination of the Applicability of the Theoretical Models for Modeling Foams

S.V. Raj
Glenn Research Center, Cleveland, Ohio

This publication replaces NASA/TM—2010-216342, June 2010.

February 2011

NASA STI Program . . . in Profile

Since its founding, NASA has been dedicated to the advancement of aeronautics and space science. The NASA Scientific and Technical Information (STI) program plays a key part in helping NASA maintain this important role.

The NASA STI Program operates under the auspices of the Agency Chief Information Officer. It collects, organizes, provides for archiving, and disseminates NASA's STI. The NASA STI program provides access to the NASA Aeronautics and Space Database and its public interface, the NASA Technical Reports Server, thus providing one of the largest collections of aeronautical and space science STI in the world. Results are published in both non-NASA channels and by NASA in the NASA STI Report Series, which includes the following report types:

- TECHNICAL PUBLICATION. Reports of completed research or a major significant phase of research that present the results of NASA programs and include extensive data or theoretical analysis. Includes compilations of significant scientific and technical data and information deemed to be of continuing reference value. NASA counterpart of peer-reviewed formal professional papers but has less stringent limitations on manuscript length and extent of graphic presentations.

- TECHNICAL MEMORANDUM. Scientific and technical findings that are preliminary or of specialized interest, e.g., quick release reports, working papers, and bibliographies that contain minimal annotation. Does not contain extensive analysis.

- CONTRACTOR REPORT. Scientific and technical findings by NASA-sponsored contractors and grantees.

- CONFERENCE PUBLICATION. Collected papers from scientific and technical conferences, symposia, seminars, or other meetings sponsored or cosponsored by NASA.

- SPECIAL PUBLICATION. Scientific, technical, or historical information from NASA programs, projects, and missions, often concerned with subjects having substantial public interest.

- TECHNICAL TRANSLATION. English-language translations of foreign scientific and technical material pertinent to NASA's mission.

Specialized services also include creating custom thesauri, building customized databases, organizing and publishing research results.

For more information about the NASA STI program, see the following:

- Access the NASA STI program home page at *http://www.sti.nasa.gov*

- E-mail your question via the Internet to *help@sti.nasa.gov*

- Fax your question to the NASA STI Help Desk at 443–757–5803

- Telephone the NASA STI Help Desk at 443–757–5802

- Write to:
  NASA Center for AeroSpace Information (CASI)
  7115 Standard Drive
  Hanover, MD 21076–1320

NASA/TM—2010-216342/REV1

Microstructural Characterization of Metal Foams: An Examination of the Applicability of the Theoretical Models for Modeling Foams

S.V. Raj
Glenn Research Center, Cleveland, Ohio

National Aeronautics and
Space Administration

Glenn Research Center
Cleveland, Ohio 44135

February 2011

Acknowledgments

The investigation was funded by NASA's Subsonic Fixed Wing Program. Discussions with Prof. John Russ, North Carolina State University, North Carolina, and Dr. Don Roth, NASA Glenn Research Center, Cleveland, Ohio, are gratefully acknowledged.

Document Change History

NASA/TM—2010-216342/REV1, February 2011

Microstructural Characterization of Metal Foams: An Examination of the Applicability of the Theoretical Models for Modeling Foams

S.V. Raj

This publication replaces NASA/TM—2010-216342, June 2010.

This report contains preliminary findings, subject to revision as analysis proceeds.

This work was sponsored by the Fundamental Aeronautics Program at the NASA Glenn Research Center.

Level of Review: This material has been technically reviewed by technical management.

Available from

NASA Center for Aerospace Information
7115 Standard Drive
Hanover, MD 21076–1320

National Technical Information Service
5301 Shawnee Road
Alexandria, VA 22312

Available electronically at http://gltrs.grc.nasa.gov

Microstructural Characterization of Metal Foams: An Examination of the Applicability of the Theoretical Models for Modeling Foams

S.V. Raj
National Aeronautics and Space Administration
Glenn Research Center
Cleveland, Ohio 44135

Abstract

Establishing the geometry of foam cells is useful in developing microstructure-based acoustic and structural models. Since experimental data on the geometry of the foam cells are limited, most modeling efforts use an idealized three-dimensional, space-filling Kelvin tetrakaidecahedron. The validity of this assumption is investigated in the present paper. Several FeCrAlY foams with relative densities varying between 3 and 15 percent and cells per mm (c.p.mm.) varying between 0.2 and 3.9 c.p.mm. were microstructurally evaluated. The number of edges per face for each foam specimen was counted by approximating the cell faces by regular polygons, where the number of cell faces measured varied between 207 and 745. The present observations revealed that 50 to 57 percent of the cell faces were pentagonal while 24 to 28 percent were quadrilateral and 15 to 22 percent were hexagonal. The present measurements are shown to be in excellent agreement with literature data. It is demonstrated that the Kelvin model, as well as other proposed theoretical models, cannot accurately describe the FeCrAlY foam cell structure. Instead, it is suggested that the ideal foam cell geometry consists of 11 faces with three quadrilateral, six pentagonal faces and two hexagonal faces consistent with the 3-6-2 Matzke cell. A compilation of 90 years of experimental data reveals that the average number of cell faces decreases linearly with the increasing ratio of quadrilateral to pentagonal faces. It is concluded that the Kelvin model is not supported by these experimental data.

1.0 Introduction

Aircraft engine noise is a major environmental concern especially in regions surrounding an airport during takeoff and landing (Ref. 1). Significant progress has been made since the advent of the first commercial jet engine-powered airplanes with current ultrahigh bypass engines being much quieter than the first generation engines. For example, the effective perceived noise level in decibels (EPNdB) relative to the International Civil Aviation Organization's (ICAO) Chapter 3 certification standards decreased from about +5 EPNdB for aircraft engines developed in the 1960s to –5 EPNdB for modern engines (Refs. 2 and 3). Despite this large improvement in engine design, there is still a great desire among policy makers and designers to reduce noise much below current levels. For example, the National Aeronautics and Space Administration (NASA) has set ambitious goals to further reduce aircraft noise by –52 db with respect to the newly adapted ICAO's Chapter 4 certification standards by the year 2020 under its Subsonic Fixed Wing (SFW) project (Ref. 4). It is expected that these noise reduction goals will be achieved through a combination of design changes and development of suitable materials (Refs. 3 and 4).

Polymeric foams have been historically used for sound absorption in several applications (Ref. 5). More recently, metal foams are being investigated for their flow resistance (Refs. 6 and 7) and sound absorption properties (Refs. 8, 9, and 10). Metal foams have been proposed for use in jet engines as acoustic treatment over rotors (Ref. 11), fan blades (Ref. 12) and other applications (Ref. 13). The acoustic and other properties of foams are dependent on their relative density, ρ^*/ρ_s, where ρ^* and ρ_s are the densities of the foam and the solid material, respectively, and microstructure (Ref. 5). Simple formulae exist for correlating relative density and some elements of the microstructure, such as, ligament length and thickness (Refs. 5, 6, 7, 8, 9, and 10). However, due to difficulties in controlling process variables, the microstructures of the foams and their properties can vary by large amounts. Although

commercially manufactured foams are specified by pores per inch (p.p.i.) and their relative densities, it is noted that the reported values of p.p.i. are not necessarily identical from one manufacturer to another (Ref. 14). For example, some vendors identify the p.p.i. of their products with that of the precursor polyurethane foam rather than the finished product without accounting for metal shrinkage during the manufacturing process.

In the case of metal foams used as acoustic liners in aircraft engines, it is important to qualitatively and quantitatively understand the role their microstructures play in affecting their acoustic and mechanical properties. Since the complex three-dimensional microstructures of the foams help to dissipate the sound energy, it is evident that a quantitative analysis of the foam microstructures would enable important correlations to be determined between the microstructural features and the gas pressure flow resistance as well as the sound absorption coefficients. These correlations are essential for developing microstructure-based models for designing acoustic liners for aircraft engines. Particularly, establishing the three-dimensional topology of the cell microstructures of foams is important effectively to model fluid flow through them and to understand their mechanical properties.

Modeling activities on foam cell structures fall into two broad categories: (a) idealized topological models based on minimizing the ratio of the surface free energy to volume free energy that can fill three-dimensional (3–D) space; and (b) engineering models based on the actual reconstruction of the 3–D foam microstructures. Among the several possible idealized topological representations of the foam microstructures (Ref. 5), the three-dimensional, space-filling Kelvin tetrakaidecahedron (Refs. 5, 15, and 16) is often favored for modeling the foam cellular network. This cell has 14 faces consisting of six squares and eight hexagonal faces. In other words, about 43 percent of the faces are squares, zero percent faces are pentagonal and 57 percent of the faces are hexagonal. It is worth noting that other topological models have been proposed, where pentagonal faces are incorporated in the cell geometry (Refs. 17 and 18). The Kelvin model assumes that all cells are all of the same size and volume so that the problem becomes one of determining the cell shape that can pack 3–D space resulting in a system with the lowest free energy (Ref. 15). In reality, cells deviate from these ideal conditions, where they may be distorted and their sizes and shapes non-uniform. Alternatively, recent computational models use actual 3–D foam microstructures as an input to the model. However, these models require the availability of high-powered computational capabilities to handle the large megabytes of input data representing the foam microstructures. The input data for these models are expensive to generate, and the models tend to be rather complex. Since foam microstructures are complex, it is necessary to develop both the relatively simple and elegant topological mathematical models, as well as, the complex, but realistic, computational engineering models in order to completely understand the microstructure-property relationships of foams.

Several investigators have tried to evaluate the 3–D shape of fat cells (Ref. 19), soap bubbles (Refs. 20 and 21), grains (Refs. 22, 23, 24, 25, 26, 27, 28, and 29) and foam cells (Refs. 30, 31, 32, and 33). The measurement techniques used in these investigations include conventional microstructural image analysis, serial section metallography, optical and x-ray micro-computerized tomography (μCT), magnetic resonance imaging (MRI), ultrasonic imaging and laser confocal microscopy (Refs. 14 and 34). Most of these procedures have advantages and disadvantages. The well-established quantitative metallography techniques (Refs. 23, 24, 25, 26, 27, 28, 29, 34, and 35) are relatively simple, inexpensive, and provide high resolution images which enable the acquisition of a large amount of statistically relevant data with relative ease. However, these procedures are destructive in nature and the 3–D information of the microstructure can only be inferred from the two-dimensional (2–D) sections using well-developed mathematical and stereological methods (Refs. 24, 25, 34, and 35). The advent of powerful computers and the availability of specialized software with capabilities to reconstruct 3–D images by “stitching” several closely-spaced 2–D images has enabled the recent development of several techniques, such as optical tomography (Ref. 21), MRI (Ref. 30) and μCT (Ref. 32), for accurately reproducing the complex 3–D foam microstructures. The primary advantages of these methods is that the resulting 3–D images along with quantitative information on the foam microstructures can provide a realistic image of the 3–D spatial distribution of the cells. In recent years, μCT is increasingly used to characterize foam microstructures due to the advantages of using 3–D reconstructed images as input to the computational engineering

models. Despite its relative popularity, it is time consuming, expensive and possesses a lower image resolution than conventional metallographic methods (Ref. 31). Typically, only a few foam cells are sampled so that the statistical sampling size is limited.

The objectives of this investigation were to characterize the microstructures of PORVAIR[1] metal foams. Quantitative information on ligament (or struts) dimensions, cell face dimensions, area fractions of open and closed faces, geometric shapes of the cell faces and distribution of ligament porosity were determined. Specifically, the present paper reports statistical data on the geometrical features of the cells faces to determine the validity of the Kelvin (Ref. 15) and other theoretical space-filling models (Refs. 16, 17, and 18) in a comprehensive manner. Other quantitative details of the foam microstructure are reported elsewhere (Ref. 36).

2.0 Experimental Procedures

Several FeCrAlY foam panels approximately 210 x 210 mm^2 in cross-sectional area and varying in thicknesses between 3.2 and 25.4 mm were procured from PORVAIR Fuel Cells Technology, Inc., Hendersonville, North Carolina. The foam panels were manufactured from precursor polyurethane foams dipped in metal powder slurries followed by sintering of the powder and burning off the polymer foams. The c.p.mm. varied between 0.2 (5 p.p.i.) and 3.9 (100 p.p.i.), whereas ρ^*/ρ_S varied between 3 and 15 percent. Square specimens ~ 25.4 x 25.4 mm in cross-sectional dimensions or 50 mm in diameter were wire electro-discharge machined from these panels for metallographic analyses. On close examination, it was observed that the microstructures of these foams are extremely complicated and difficult to characterize. The foam microstructures consisted of interconnected cells randomly stacked in a three-dimensional array with the cell boundaries moving in and out of the field of view.

Preliminary attempts to study the shapes of the foam cells using either μCT with resolutions varying between 20 and 100 μm or an automated serial sectioning[2] of a FeCrAlY foam specimen and the subsequent 3–D reconstruction of the 2–D sectioned images proved to be unsatisfactory since the cell outline could not be clearly defined in the images. Instead, macrophotographs were obtained of the as-received foam specimens (Fig. 1(a)). This technique allowed a 3–D visualization of the foam microstructure with several adjacent faces of a cell being clearly demarcated (Fig. 1(b)). It is noted that Figure 1(a) is similar to the 3–D reconstructed image of polymer foams (Ref. 31) except that the present imaging technique is faster and cheaper. Quantitative metallographic measurements were conducted on 6 to 7 randomly selected areas for each foam specimen and a large number of faces were measured to ensure that the measurements were representative and to minimize measurement errors. The number of edges per face was counted by assuming that the faces could be approximated by regular polygons with the number of cell faces measured varying between 207 for foams 0.2 c.p.mm. to 745 for 3.9 c.p.mm. This assumption was not always valid since some faces were either circular or elliptical rather than polygonal and the edges were often curved. In some instances, the edges of a face curved out of the plane of view. In addition, two adjacent edges did not meet always at a relatively sharp point but had a significant curvature, while adjacent faces met at triple surfaces rather than triple points in many instances. These issues complicated the measurements and they are likely to add to the errors in measurements. Nevertheless, by measuring a large number of faces, it was felt that the errors in measurement would be minimized. It is noted that a similar method was used by Montminy et al. (Ref. 31) to analyze 3–D μCT images.

[1]PORVAIR is the trademark of PORVAIR Fuel Cells Technology, Hendersonville, North Carolina.
[2]The automated sectioning of the FeCrAlY foams and the 3–D image reconstruction was conducted by UES, Inc., Dayton, Ohio.

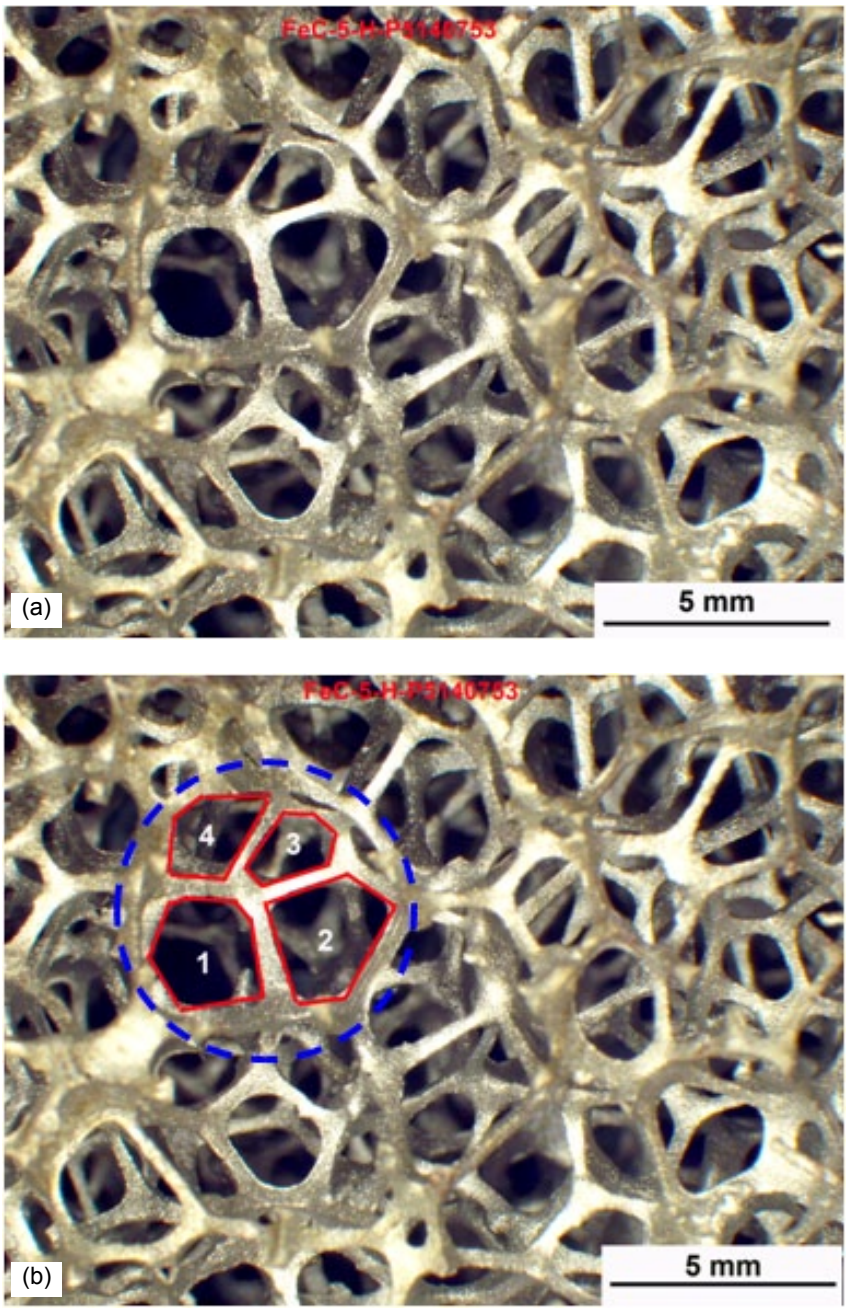

Figure 1.—(a) Optical macrograph of a FeCrAlY foam with a nominal pore density of 0.2 c.p.mm. (5 p.p.i) and ρ^*/ρ_s = 3.3 percent; (b) polygonal representations of the faces, 1, 2, 3 and 4 enclosed by the broken circle belong to the same cell.

3.0 Results and Discussion

Figures 1(a) shows an optical macrograph of a FeCrAlY foam specimen with a nominal cell density of 0.2 c.p.mm. (5 p.p.i.) and ρ^*/ρ_S = 3.3 percent; Figure 1(b) shows the corresponding polygonal representations of the faces. The numbers identify the faces for tracking purposes. The complex nature of the foam microstructures is self evident in these figures. On close examination, it was observed that several neighboring faces were part of the same cell. For example, the faces numbered 1, 2, 3 and 4

enclosed by the broken circle represent the outer faces a single cell with some of the inner faces of the cell visible in the background (Fig. 1(b)). The volume fractions of the open cells decreased while that of the closed cells increased with increasing relative density. Since it was often difficult to clearly discern the boundaries of closed faces, only the shapes of the open faces were demarcated in these measurements in order to minimize errors in measurement. The cells were generally equiaxed irrespective of c.p.mm. and relative density.

Figures 2(a) to (d) show the frequency histogram and cumulative frequency plots of the number of edges per face for four FeCrAlY foams. An examination of Figures 2(a) to (d)clearly establishes that 97 percent of the faces were either four, n_4, five, n_5, or six, n_6,-sided with over 50 percent of the faces being five-sided. Less than 1 percent of the faces were triangular and less than 2 percent were heptagonal except in the case of foams with 2.4 c.p.mm (60 p.p.i), which had about 4 percent heptagonal faces. The average values of the number of edges per face, $\overline{N}$, were determined to be 4.9 ± 0.7, 5.0 ± 0.8, 4.9 ± 0.8, and 4.9 ± 0.8 for the FeCrAlY foams with actual values of ρ^*/ρ_S being 3.3 percent (0.2 c.p.mm.), 9.5 percent (2.4 c.p.mm.), 10.1 percent (3.1 c.p.mm.) and 9.3 percent (3.9 c.p.mm.), respectively. The errors represent 95 percent confidence levels. Significantly, these observations were not influenced by either the relative densities of the foams or the lineal cell densities.

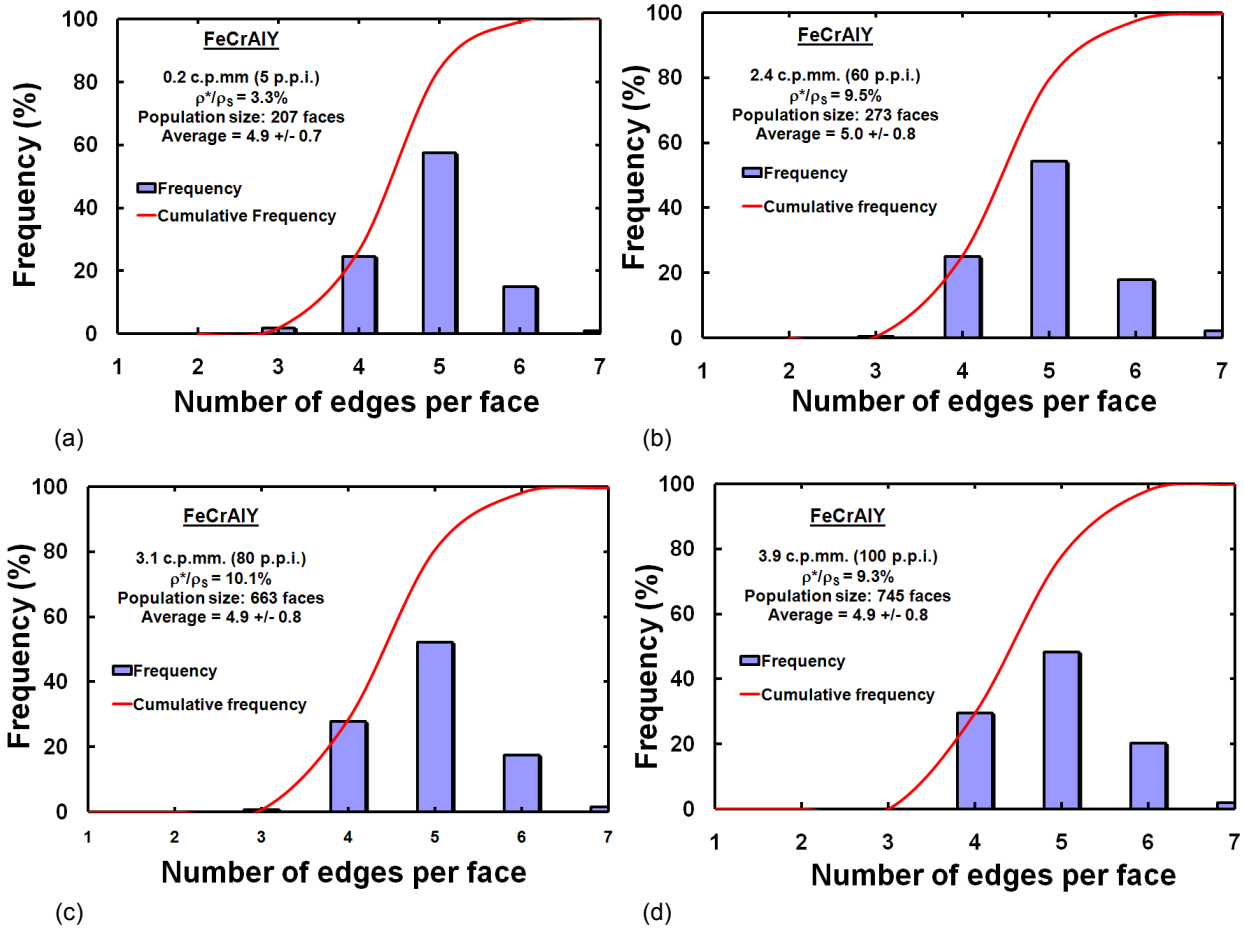

Figure 2.—Frequency histograms and cumulative frequencies showing the distributions of the number of edges per face for FeCrAlY foams with different values of cells per mm and relative densities.

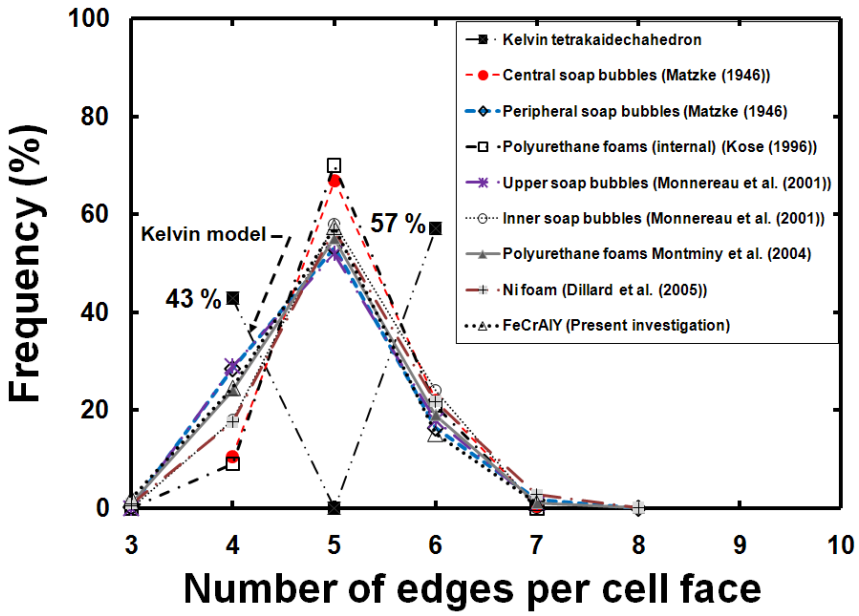

Figure 3.—Comparison of the frequency histograms of the distributions of the number of edges per face for soap bubbles (Refs. 20 and 21), polyurethane foams (Refs. 30 and 31), Ni foam (Refs. 32) and a FeCrAlY foam with 0.2 c.p.mm. (5 p.p.i.) and ρ^*/ρ_s = 3.3 percent. The solid squares and associated legends represent the theoretical values for the Kelvin tetrakaidechedron.

Figure 3 compares the present results with similar measurements on soap bubbles (Refs. 20 and 21), polyurethane foams (Refs. 30 and 31) and Ni foam (Ref. 32). These literature data include measurements conducted on both surface and internal cells using different measurement techniques. Table 1 compares the percentages of four, five, and six-sided faces observed on the FeCrAlY foams with those reported for fat cells (Ref. 19), soap bubbles (Refs. 20, 21, and 22), β-brass grains (Ref. 22), and foams (Refs. 22, 30, 31, and 32). It is noted that the data compiled in Table 1 were obtained by several different techniques ranging from simple visual observations to complex NMR and μCT 3–D scans over a 90-year period. Significantly, in all cases, more than 50 percent of the cell faces had a pentagonal geometry irrespective of the material and measuring technique used (Table 1 and Fig. 3). The present results fall well within the range of other observations reported in the literature.

An examination of Figure 3 shows that the Kelvin tetrakaidecahedron model (Ref. 15), which predicts 0 percent five-sided faces, is inconsistent with the experimental observations. The fact that the Kelvin model fails to be consistent with the experimental results is not surprising. This model is based on a mathematical conjecture that soap bubbles and foam microstructures can be ideally represented by dividing three-dimensional space into cells of equal volume in a manner that follows Plateau's rules for mechanical equilibrium and minimization of the surface area (Ref. 37). It is noted that the Kelvin model requires the arrangement of tetrakaidecahedron cells to be topologically ordered and spatially periodic to fill space. Real foams are far from this ideal configuration since factors, such as residual stresses due to processing methods, topological disorder (Ref. 37), unequal cell volumes, aperiodic spatial ordering of the cells (Ref. 20), and thick ligaments and triple points, can influence the cell topology. Matzke (Ref. 20) studied 400 peripheral soap bubbles and observed that the largest number of them possessed 11-hedra cells with three four-sided, six five-sided and two six-sided faces (3-6-2)[3] (Fig. 4). However, these soap bubbles only constituted 17 percent of the total number of bubble studied since 20 other shapes were observed. In contrast, 97 percent of the cell faces in the FeCrAlY foams were either four, five or six-

[3]This nomenclature of identifying the cells was suggested by Kraynik et al. (Ref. 37].

sided. Therefore, it would be interesting to determine the number of faces for the ideal cell representing the microstructures of the FeCrAlY foams.

TABLE 1.—COMPARISON OF THE PERCENTAGES OF FOUR, FIVE AND SIX-SIDED FACES OBSERVED IN FeCrAlY FOAMS WITH OBSERVATIONS ON FAT CELLS (REF. 19), SOAP BUBBLES (REFS. 20, 21, AND 22), β-BRASS GRAINS (REF. 22), AND FOAMS (REFS. 22, 30, 31, AND 32)

Description	Measurement technique	Percentage of polyhedral faces, n_4, n_5 and n_6
Fat cells (Lewis (Ref. 19))	Optical microscopy or visual	$n_4 = 21\%$; $n_5 = 53\%$; $n_6 = 23\%$
Soap bubbles (Matzke (Ref. 20))	Optical microscopy	Peripheral: $n_4 = 29\%$; $n_5 = 53\%$; $n_6 = 16\%$; Central: $n_4 = 11\%$; $n_5 = 67\%$; $n_6 = 22\%$
Soap bubbles (Monnereau et al. (Ref. 21))	Optical tomography	Upper bubbles; $n_4 = 29\%$; $n_5 = 52\%$; $n_6 = 18\%$; Internal bubbles: $n_4 = 18\%$; $n_5 = 58\%$; $n_6 = 24\%$
β-brass grains Soap bubbles Ammonium oleate foams Gelatin foams (Desch (Ref. 22))	Visual	$n_4 = 20\%$; $n_5 = 44\%$; $n_6 = 28\%$ $n_4 = 20\%$; $n_5 = 50\%$; $n_6 = 22\%$ $n_4 = 21\%$; $n_5 = 50\%$; $n_6 = 25\%$ $n_4 = 19$-38%; $n_5 = 32$-57%; $n_6 = 10$-25%
Polyurethane foams (Kose (Ref. 30)) (Montminy et al. (Ref. 31))	 NMR μCT	 $n_4 = 9\%$; $n_5 = 70\%$; $n_6 = 21\%$ $n_4 = 24\%$; $n_5 = 55\%$; $n_6 = 19\%$
Open cell Ni foam (Dillard et al. (Ref. 32))	μCT	$n_4 = 18\%$; $n_5 = 57\%$; $n_6 = 22\%$
FeCrAlY foams (Present investigation)	Optical microscopy	$n_4 = 25\%$; $n_5 = 57\%$; $n_6 = 15\%$ (0.2 c.p.mm.; $\rho^*/\rho_s = 3.3\%$)
		$n_4 = 24\%$; $n_5 = 54\%$; $n_6 = 18\%$ (2.4 c.p.mm.; $\rho^*/\rho_s = 9.5\%$)
		$n_4 = 28\%$; $n_5 = 52\%$; $n_6 = 18\%$ (3.1 c.p.mm.; $\rho^*/\rho_s = 10.1\%$)
		$n_4 = 26\%$; $n_5 = 50\%$; $n_6 = 22\%$ (3.9 c.p.mm.; $\rho^*/\rho_s = 9.3\%$)

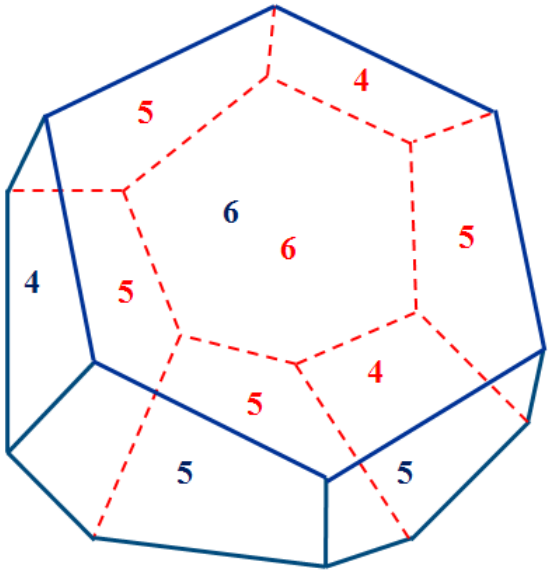

Figure 4.—A 3-6-2 11-hydra cell with three quadrilateral, six pentagonal and two hexagonal faces (Ref. 20). The numbers represent the number of edges enclosing the cell face. The blue solid lines representing the forward faces are identified by the blue lettering, while the red broken lines representing the back faces are identified by the red lettering.

Since quantitative optical metallography gives 2–D information, the 3–D topographical characteristics of the microstructure can be determined from well established stereology equations (Refs. 23, 24, 25, 26, 27, 28, 29, 34, 35, 38, 39, and 40). The number of faces per cell, ***F***, the number of edges per cell, ***E***, and the number of vertices per cell, ***V***, of the 3–D cell are related by the Euler equation (Refs. 5, 25, 34, and 39) and they can be determined from $\overline{N}$ using the Coxeter equations (Ref. 41)

$$\boldsymbol{F} = \frac{12}{\left[6 - \overline{N}\right]} \tag{1a}$$

$$\boldsymbol{E} = \frac{6\overline{N}}{\left[6 - \overline{N}\right]} \tag{1b}$$

$$\boldsymbol{V} = \frac{4\overline{N}}{\left[6 - \overline{N}\right]} \tag{1c}$$

Table 2 shows the calculated values of ***F***, ***E***, ***V***, and the corresponding experimental values of N_4, N_5 and N_6 for the four FeCrAlY foams.[4] Using the measured values of $\overline{N}$, the corresponding values of ***F*** calculated from equation (1a) are 11.0, 11.7, 11.1 and 11.4 for foams with 0.2 (5 p.p.i.), 2.4 (60 p.p.i.), 3.1 (80 p.p.i.) and 3.9 c.p.mm. (100 p.p.i.), respectively. Based on these results, the topological characteristics of the ideal PORVAIR foam cell are: ***F*** = 11, ***E*** = 27 and ***V*** = 18, which satisfy Euler's theorem (i.e., ***V*** – ***E*** + ***F*** = 2) with N_4 = 3, N_5 = 6 and N_6 = 2. These values are independent of relative density.

TABLE 2.—CALCULATED VALUES OF *F*, *E*, *V*, N_4, N_5 AND N_6 FOR FeCrAlY FOAMS

Linear cell density (c.p.mm)	ρ^*/ρ_s (%)	*F*	*E*	*V*	N_4	N_5	N_6
0.2 (5 p.p.i.)	3.3	11.0	26.7	17.8	3	6	2
2.4 (60 p.p.i.)	9.5	11.7	30.0	20.0	3	6 or 7	2
3.1 (80 p.p.i.)	10.1	11.1	26.7	17.8	3	6	2
3.9 (100 p.p.i.)	9.3	11.4	26.7	17.8	3	6	2 or 3
	Average	11.3	27.5	18.4	3	6	2

Table 3 compares the topological features of the FeCrAlY foams with several simple cell shapes (Ref. 5), where **C** is the number of cells. The topological characteristics of the FeCrAlY foams do not agree with any of these simple geometries. Instead, they appear to be closer to the topological structure of clathrates although more detailed topological modeling needs to be conducted to establish this possibility (Refs. 42 and 43). As noted above, Matzke (Ref. 20) observed that most of the peripheral soap bubbles were eleven-hedra cells with three four-sided, six five-sided and two six-sided faces (3-6-2). Based on the excellent agreement between the present results and Matzke's data on peripheral soap bubbles (Ref. 20) (Fig. 3) taken together with the fact that the total number of faces for the FeCrAlY foams was determined to be 11 (Table 2), it is reasonable to suggest that the 11-hedra 3-6-2 cell is the most representative of the FeCrAlY foam cellular structure.

Table 4 shows the predicted (Refs. 15, 16, 17, and 18) and the experimental (Refs. 20, 21, and 30) percentage distributions of polyhedral faces and the average number of faces per cell, $\boldsymbol{F}_{average}$. As noted earlier, the data were obtained by different methods on several materials over a 90-year period. The average value of F = 11.3 determined for the FeCrAlY foam cells (Table 2) is in very good agreement with the experimental observations on the peripheral (Ref. 20) or upper (Ref. 21) soap bubbles and gelatin foams (Ref. 22) for which the average number of faces is about 11.

[4]In this paper, n_i represents the percentage of faces with i edges, whereas N_i is number of such faces enclosing the cell.

TABLE 3.—COMPARISON OF THE GEOMETRIC PROPERTIES OF FeCrAlY FOAM CELLS WITH THOSE FOR SIMPLE POLYHEDRA (REF. 5)

Cell shape	Number of face shapes				*F*	*E*	*V*	*C*	Remarks
	3	4	5	6					
Tetrahedron	4	--	--	--	4	6	4	1	Regular Platonic solid
Triangular prism	2	3	--	--	5	9	6	1	Packs to fill space
Square Prism	--	6	--	--	6	12	8	1	Packs to fill space
Hexagonal Prism	--	6	--	2	8	18	12	1	Packs to fill space
Octahedron	8	--	--	--	8	12	6	1	Regular Platonic solid
Rhombic Dodecahedron	--	12	--	--	12	24	14	1	Packs to fill space
Pentagonal Dodecahedron	--	--	12	--	12	30	20	1	Regular Platonic solid
Tetrakaidecahedron	--	6	--	8	14	36	24	1	Packs to fill space
Icosahedron	20	--	--	--	20	30	12	1	Regular Platonic solid
3-6-2 cell	--	3	6	2	11	27	18	1	FeCrAlY foam (present investigation)

TABLE 4.—COMPARISON OF THE GEOMETRIC PROPERTIES OF THE CELLS PREDICTED BY SEVERAL THEORETICAL MODELS (REFS. 15, 16, 17, AND 18) AND EXPERIMENTAL DATA (REFS. 20, 21, 22, 30, 31, AND 32)

Description	Percentage of polyhedral faces, n_4, n_5 and n_6	$F_{average}$
Kelvin cell (Ref. 15)	$n_4 = 43\%$; $n_5 = 0\%$; $n_6 = 57\%$	14
Williams cell (Ref. 17)	$n_4 = 14\%$; $n_5 = 57\%$; $n_6 = 29\%$	14
Weaire and Phelan model (Refs. 16 and 18)	$n_4 = 0\%$; $n_5 = 89\%$; $n_6 = 11\%$	13.4
Soap bubbles (Matzke (Ref. 20))	Peripheral: $n_4 = 29\%$; $n_5 = 53\%$; $n_6 = 16\%$ Central: $n_4 = 11\%$; $n_5 = 67\%$; $n_6 = 22\%$	11.0 (peripheral) 13.7 (central)
Soap bubbles (Monnereau et al. (Ref. 21))	Upper bubbles: $n_4 = 29\%$; $n_5 = 52\%$; $n_6 = 18\%$ Internal bubbles: $n_4 = 18\%$; $n_5 = 58\%$; $n_6 = 24\%$	11.1 (upper bubbles) 13.5 (internal bubbles)
β-brass grains Soap bubbles Ammonium oleate foams Gelatin foams (Desch (Ref. 22))	$n_4 = 20\%$; $n_5 = 44\%$; $n_6 = 28\%$ $n_4 = 20\%$; $n_5 = 50\%$; $n_6 = 22\%$ $n_4 = 21\%$; $n_5 = 50\%$; $n_6 = 25\%$ $n_4 = 19$-38%; $n_5 = 32$-57%; $n_6 = 10$-25%	14.5 13.0 13.0 9.0-11.0
Polyurethane foam (Kose (Ref. 30)) (Montminy et al. (Ref. 31))	 $n_4 = 9\%$; $n_5 = 70\%$; $n_6 = 21\%$ $n_4 = 24\%$; $n_5 = 55\%$; $n_6 = 19\%$	 13.6 13.0
Open cell Ni foam (Dillard *et al*. (Ref. 32))	$n_4 = 17.6\%$; $n_5 = 56.8\%$; $n_6 = 21.8\%$	13.0
FeCrAlY foams (Present investigation)	$n_4 = 24$-28%; $n_5 = 50$-57%; $n_6 = 15$-22%	11.3

A close examination of Table 4 reveals that the present results do not agree with the predictions of the three topological models (Refs. 15, 16, 17, and 18). The Kelvin cell (Ref. 15) does not possess any pentagonal faces, whereas the Weaire-Phelan model (Refs. 16, 18, and 30) does not have any quadrilateral faces, with the total number of faces being either 14 or 13.4, respectively. The Williams cell (Ref. 17) with 14 faces possesses 14 percent quadrilateral, 57 percent pentagonal and 29 percent hexagonal faces. However, this model also does not agree with the present observations on the FeCrAlY foams. This difference between the experimental results and the theoretical predictions is to be expected since theoretical efforts mainly consider the surface and volume free energy contributions to the total free energy (Ref. 37). As indicated earlier, other factors can influence the final cell topology of real foams. For example, the effects of residual stresses developed in the foam panels during processing have not included in these theoretical derivations. Qualitatively, one can modify the Gibbs free energy equation as follows:

$$\Delta G = (\Delta g_v + \Delta g_e) \cdot V_C + \Delta g_s \cdot S_C \tag{2}$$

where, ΔG, Δg_v, Δg_e and Δg_s are the changes in the total, volume, residual strain and surface Gibbs free energies, respectively, V_C is the cell volume and S_C is the surface are of the cell. It is important to note that current theoretical models agree incorrectly assume that $\Delta g_e = 0$ for real foams.

Table 4 shows that $\boldsymbol{F}_{average}$ varied between 9.0 and 14.5 (Refs. 20, 21, 22, and 30). On further examination of the data, $\boldsymbol{F}_{average}$ decreases linearly with the increasing ratio, n_4/n_5, (Fig. 5(a))

$$\boldsymbol{F}_{average} = -5.1(n_4/n_5) + 14.3 \qquad (R_d^2 = 0.461) \tag{3}$$

where R_d^2 is the coefficient of determination. In contrast, it is independent of n_6/n_5 (Fig. 5(b)). The regression Equation (3) is represented by the solid line in Figure 5(a); the broken horizontal line in Figure 5(b) represents the average value of $\boldsymbol{F}_{average} = 12.2$ for all the data. Equation (3) predicts a value of $\boldsymbol{F}_{average} = 14.3$ for $n_4 = 0$, $\boldsymbol{F}_{average} = 9.2$ for $n_4 = n_5$, and $\boldsymbol{F}_{average} = \infty$ for $n_5 = 0$. Thus, the Kelvin model, for which $n_5 = 0$, is not supported by the trend in the experimental data.

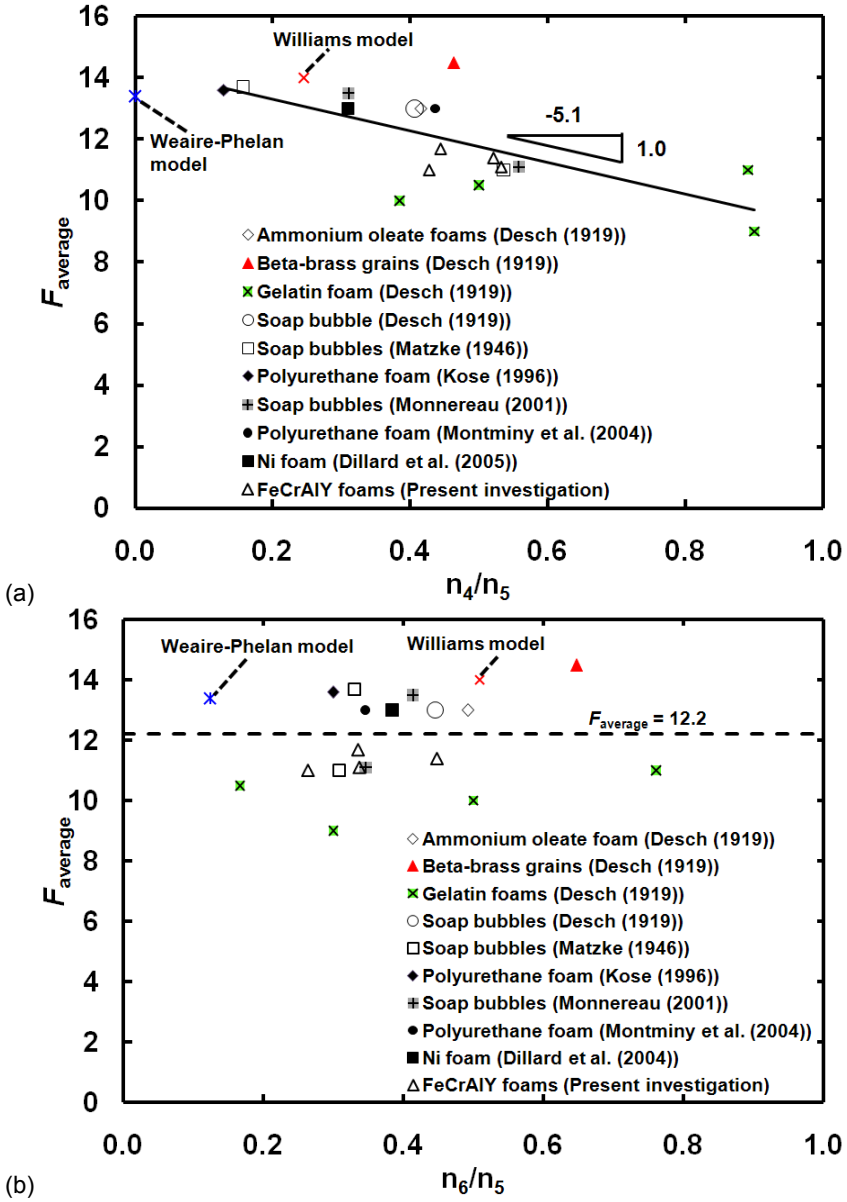

Figure 5.—Variation of the average number of cell faces against the ratio of (a) quadrilateral to pentagonal, and (b) hexagonal to pentagonal faces. The regression line through the data is represented by the solid line in (a). The present data on FeCrAlY foams are compared with literature data (Refs. 20, 21, 22, 30, 31, and 32).

4.0 Summary and Conclusions

A detailed microstructural analysis of several FeCrAlY metal foams with relative densities varying between 3 and 15 percent, and linear cell densities varying between 0.2 and 3.9 c.p.mm., was conducted to evaluate the topology of the foam cells. The shapes of cell faces were evaluated by approximating the faces by regular polygons. It was observed that between 24 and 28 percent of the cell faces were quadrilateral, 50 to 57 percent pentagonal, and 15 to 22 percent hexagonal in morphology. The present results are in excellent agreement with observations on soap bubbles (Refs. 20 and 21). Based on Matzke's observations (Ref. 20), it is suggested that the FeCrAlY foam cells had a total of 11 faces with three quadrilateral, six pentagonal and two hexagonal faces. Both sets of results do not agree with the 14-hedra Kelvin tetrakaidecahedron model (Ref. 15), which only has 43 and 57 percent quadrilateral and hexagonal faces, respectively. Neither do the present results agree with the Williams (Ref. 17) and Weaire-Phelan models (Refs. 16, 18, and 30) models. The present calculations show that the 3-6-2 cell, which probably best describes the FeCrAlY foam cells, has 27 edges and 18 vertices. A compilation of 90 years of experimental data reveals that the average number of cell faces decreases linearly with the increasing ratio of quadrilateral to pentagonal faces. It is concluded that the Kelvin model is not supported by these experimental data.

References

1. J.L. Kerrebrock: *Aircraft Engines and Gas Turbines*, The MIT Press, Cambridge, MA, Ch. 9, 1992.
2. B.L. Koff: "Gas Turbine Technology Evolution: A Designer's Perspective," *J. Propulsion Power*, Vol. 20, 2004, pp. 577–595.
3. D.L. Huff and E. Envia: "Jet Engine Noise Generation, Prediction, and Control," *Handbook of Noise and Vibration Control*, edited by M. J. Crocker, John Wiley, Hoboken, NJ, 2007, pp. 1090–1102.
4. E. Envia and R. Thomas: "Research Progress in Aircraft Noise Research," ARMD Technical Seminar October 16, 2007, http://ntrs.nasa.gov/archive/nasa/casi.ntrs.nasa.gov/20080006600_2008004016.pdf, NASA Glenn Research Center, Cleveland, OH, 2007.
5. L.J. Gibson and M.F. Ashby: *Cellular Solids*, Cambridge University Press, Cambridge, U.K., 1997.
6. C.Y. Zhao, T. Kim, T.J. Lu and H.P. Hodson: "Thermal Transport Phenomena in Porvair Metal Foams and Sintered Beds," Final Report, August 2001, Micromechanics Centre & Whittle Lab., Department of Engineering, University of Cambridge, Cambridge, U.K., 2001.
7. T.J. Lu, M. Kepets and A.P. Dowling: "Acoustic Properties of Sintered FeCrAlY Foams with Open Cells (I): Static Flow Resistance," *Sci. China Ser E-Tech Sci*., 2008, Vol. 51, 1803–1811.
8. T.J. Lu, A. Hess and M.F. Ashby: "Sound Absorption in Metal Foams," *J. Appl. Phys.*, Vol. 85, 1999, pp. 7528–7539.
9. T.J. Lu, F. Chen and D. He: "Sound Absorption of Cellular Metals with Semiopen Cells," *J. Acoustic. Soc. Am.*, Vol. 108, 2000, pp. 1697–1709.
10. T.J. Lu, M. Kepets and A.P. Dowling: "Acoustic Properties of Sintered FeCrAlY Foams with Open Cells (II): Sound Attenuation," *Sci. China Ser E-Tech Sci*., 2008, Vol. 51, pp. 1812–1837.
11. D.L. Sutliff, D.M. Elliott, M.G. Jones, and T.C. Hartley: "Attenuation of FJ44 Turbofan Engine Noise With a Foam-Metal Liner Installed Over-the-Rotor," NASA/TM—2009-215666, NASA Glenn Research Center, Cleveland, OH, 2009.
12. S.V. Raj, L.J. Ghosn, B.A. Lerch, M. Hebsur, L.M. Cosgirff and M. Topolski: "An Evaluation of Lightweight 17-4PH Stainless Steel Foam Design Concepts for Fan and Propeller Blade Applications," NASA/TM—2005-213620, NASA Glenn Research Center, Cleveland, OH, 2005.
13. W.E. Azzi, W.L. Roberts and A. Rabiei: "Developing an Application for Refractory Open Cell Metal Foams in Jet Engines," *Mater. Res. Soc. Symp. Proc.*, Vol. 851, 2005, p. NN11.3.
14. S. Mullens, J. Luyten and J. Zeschky: "Characterization of Structure and Morphology," *Cellular Ceramics: Structure, Manufacturing, Properties and Applications*, edited by M. Scheffler and P. Colombo, Wiley-VCH Verlag GmbH & Co. KGaA, 2005, pp. 227–266.

15. W. Thompson: “On the Dimension of Space with Minimum Partitional Area,” *Phil. Mag.*, Vol. 24, 1887, pp. 503–514.
16. D. Weaire and S. Hutzler: *The Physics of Foams*, Oxford University Press, Oxford, U.K., 1999.
17. R.E. Williams: “Space-Filling Polyhedron: Its Relation to Aggregates of Soap Bubbles, Plant Cells, and Metal Crystallites,” *Science*, Vol. 161, 1968, pp. 276–277.
18. D. Weaire and R. Phelan: “The Structure of Monodisperse Foam,” *Phil. Mag. Lett.*, Vol. 70, 1994, pp. 345–350.
19. F.T. Lewis: “A Further Study of the Polyhedral Shapes of Cells,” *Amer. Acad. Arts Sci.*, Vol. 61, 1925, pp. 1–34.
20. E.B. Matzke: “The Three-Dimensional Shape of Bubbles in Foam – An Analysis of the Role of Surface Forces in Three-Dimensional Cell Shape Determination,” *Amer. J. Botany*, Vol. 33, 1946, pp. 58–80.
21. C. Monnereau, B. Prunet-Foch, and M. Vignes-Adler: “Topology of Slightly Polydisperse Real Foams,” *Phys. Rev. E*, Vol. 63, 2001, p. 061402.
22. C.H. Desch: “The Solidification of Metals from the Liquid State,” *J. Inst. Metals*, Vol. 22, 1919, pp. 241–266.
23. D. Harker and E.R. Parker: “Grain Shape and Grain Growth,” *Trans. ASM*, Vol. 34, 1945, pp. 156–201.
24. C.S. Smith: “Introduction to Grains, Phases, and Interfaces-an Interpretation of Microstructure,” *Trans. AIME*, Vol. 175, 1948, pp. 15–51.
25. C.S. Smith: “Grain Shapes and Other Metallurgical Applications of Topology,” *Metal Interfaces*, American Society for Metals, Cleveland, OH, 1952, pp. 63–113.
26. C.S. Smith: “Structure, Substructure, Superstructure,” *Rev. Modern Phys.*, Vol. 36, 1964, pp. 524–532.
27. D.A. Aboav and T.G. Langdon: “The Shape of Grains in a Polycrystal,” *Metallography*, Vol. 2, 1969, pp. 171–178.
28. K. Ejiri: “Grain Shapes in Two-Dimensional Sections of Sintered Bodies,” *J. Cryst. Growth*, Vol. 19, 1973, pp. 77–78.
29. M.D. Higgins: “Measurement of Crystal Size Distributions,” *Amer. Mineralog.*, Vol. 85, 2000, pp. 1105–1116.
30. K. Kose: “3D NMR Imaging of Foam Structures,” *J. Magnet. Resonance*, Vol. A 118, 1996, pp. 195–201.
31. M.D. Montminy, A. R. Tannenbaum and C. W. Macosko: “The 3D Structure of Real Polymer Foams,” *J. Colloid Interface Sci.*, Vol. 280, 2004, pp. 202–211.
32. T. Dillard, F. N’Guyen, E. Maire, L. Salvo, S. Forest, Y. Bienvenu, J. D. Bartout, M. Croset, R. Denievel and P. Cloetens: “3D Quantitative Image Analysis of Open-Cell Nickel Foams Under Tension and Compression Loading Using X-ray Microtomography,” *Phil. Mag.*, Vol. 85, 2005, pp. 2147–2175.
33. A.P. Roberts: “Modeling Structure-Property Relationships in Random Cellular Materials,” *Cellular Ceramics: Structure, Manufacturing, Properties and Applications*, edited by M. Scheffler and P. Colombo, Wiley-VCH Verlag GmbH & Co. KGaA, 2005, pp. 267–288.
34. J.C. Russ and R. DeHoff: *Practical Stereology*, Kluwer Academic/Plenum Publishers, New York, N.Y., 2000.
35. R.T. DeHoff and G.Q. Liu: “On the Relation between Grain Size and Grain Topology,” *Metall. Trans.*, Vol. 16A, 2007, pp. 1985–2011.
36. S.V. Raj and J.A. Kerr: “Effect of Microstructural Parameters on the Relative Densities of Metal Foams,” Metall. Mater. Trans. A, doi: 10.1007/s11661-010-0573-z.
37. A.M. Kraynik, D.A. Reinelt and F.V. Swol: “Structure of Random Foam,” *Phys. Rev. Lett.*, Vol. 93, 2004, p. 208301.
38. C.S. Smith and L. Guttman: “Measurement of Internal Boundaries in Three-Dimensional Structures by Random Sectioning,” *Trans. AIME*, Vol. 197, 1953, pp. 81–87.

39. C.S. Smith: “Microstructure,” *Trans. ASM*, Vol. 45, 1953, pp. 533–575.
40. T.D. Peterson: “A Refined Technique for Measuring Crystal Size Distributions in Thin Section,” *Contrib. Mineral Petrol*, Vol. 124, 1996, pp. 395–405.
41. H.S. M. Coxeter: “Close-Packing and Froth,” *Illinois J. Math*, Vol. 2, 1958, pp. 746–758.
42. V. I. Kosyakov: “Topology of Polyhedral Clathrate Frameworks. 2. Frameworks Constructed of Polyhedral Stories,” *J. Struct. Chemistry*, Vol. 37, 1996, pp. 106–113.
43. H. Tomono, H. Eguchi, and K. Tsumuraya: “Binding Between Endohedral Na atoms in Si Clathrate I; A First Principles Study,” *Journal of Physics: Condensed Matter*, Vol. 20, 2008, p. 385209, doi:10.1088/0953-8984/20/38/385209.

REPORT DOCUMENTATION PAGE	Form Approved OMB No. 0704-0188

1. REPORT DATE *(DD-MM-YYYY)*	2. REPORT TYPE	3. DATES COVERED *(From - To)*
01-02-2011	Technical Memorandum	

4. TITLE AND SUBTITLE
Microstructural Characterization of Metal Foams: An Examination of the Applicability of the Theoretical Models for Modeling Foams

5a. CONTRACT NUMBER

5b. GRANT NUMBER

5c. PROGRAM ELEMENT NUMBER

6. AUTHOR(S)
Raj, S., V.

5d. PROJECT NUMBER

5e. TASK NUMBER

5f. WORK UNIT NUMBER
WBS 561581.02.08.03.15.12

7. PERFORMING ORGANIZATION NAME(S) AND ADDRESS(ES)
National Aeronautics and Space Administration
John H. Glenn Research Center at Lewis Field
Cleveland, Ohio 44135-3191

8. PERFORMING ORGANIZATION REPORT NUMBER
E-17279-1

9. SPONSORING/MONITORING AGENCY NAME(S) AND ADDRESS(ES)
National Aeronautics and Space Administration
Washington, DC 20546-0001

10. SPONSORING/MONITOR'S ACRONYM(S)
NASA

11. SPONSORING/MONITORING REPORT NUMBER
NASA/TM-2010-216342-REV1

12. DISTRIBUTION/AVAILABILITY STATEMENT
Unclassified-Unlimited
Subject Categories: 05, 07, 23, 26, and 31
Available electronically at http://www.sti.nasa.gov
This publication is available from the NASA Center for AeroSpace Information, 443-757-5802

13. SUPPLEMENTARY NOTES
This publication replaces NASA/TM—2010-216342, June 2010.

14. ABSTRACT
Establishing the geometry of foam cells is useful in developing microstructure-based acoustic and structural models. Since experimental data on the geometry of the foam cells are limited, most modeling efforts use an idealized three-dimensional, space-filling Kelvin tetrakaidecahedron. The validity of this assumption is investigated in the present paper. Several FeCrAlY foams with relative densities varying between 3 and 15 percent and cells per mm (c.p.mm.) varying between 0.2 and 3.9 c.p.mm. were microstructurally evaluated. The number of edges per face for each foam specimen was counted by approximating the cell faces by regular polygons, where the number of cell faces measured varied between 207 and 745. The present observations revealed that 50 to 57 percent of the cell faces were pentagonal while 24 to 28 percent were quadrilateral and 15 to 22 percent were hexagonal. The present measurements are shown to be in excellent agreement with literature data. It is demonstrated that the Kelvin model, as well as other proposed theoretical models, cannot accurately describe the FeCrAlY foam cell structure. Instead, it is suggested that the ideal foam cell geometry consists of 11 faces with three quadrilateral, six pentagonal faces and two hexagonal faces consistent with the 3-6-2 Matzke cell. A compilation of 90 years of experimental data reveals that the average number of cell faces decreases linearly with the increasing ratio of quadrilateral to pentagonal faces. It is concluded that the Kelvin model is not supported by these experimental data.

15. SUBJECT TERMS
Metal foams; Acoustic models; Foam cell topology; Kelvin cell

16. SECURITY CLASSIFICATION OF:			17. LIMITATION OF ABSTRACT	18. NUMBER OF PAGES	19a. NAME OF RESPONSIBLE PERSON
a. REPORT	b. ABSTRACT	c. THIS PAGE			STI Help Desk (email:help@sti.nasa.gov)
U	U	U	UU	19	19b. TELEPHONE NUMBER *(include area code)* 443-757-5802